Biochimica et Biophysica Acta, 722 (1983) 23–35
Elsevier Biomedical Press

BBA 41202

PRIMARY PHOTOCHEMISTRY OF PHOTOSYSTEM I IN CHLOROPLASTS

DYNAMICS OF REVERSIBLE CHARGE SEPARATION IN OPEN REACTION CENTERS AT 25 K

MARK S. CROWDER and ALAN BEARDEN

Department of Biophysics and Medical Physics, and Division of Biology and Medicine, Lawrence Berkeley Laboratory, University of California, Berkeley, CA 94720 (U.S.A.)

(Received April 6th, 1982)
(Revised manuscript received August 18th, 1982)

Key words: Photosystem I; Reaction center; Charge separation; P-700; ESR

The reduction rate of oxidized reaction center chlorophyll of Photosystem I after laser-flash excitation at 25 K has been determined for D-144 subchloroplast fragments and chloroplasts. A maximum of 40% of Photosystem I reaction centers undergo irreversible charge separation (P-700, Cluster A: $P\text{-}700^+$, Cluster A^-) at 25 K, a percentage which is independent of laser-flash intensity. The remaining reaction centers in chloroplasts and D-144 fragments undergo reversible charge separation with biphasic recombination. Similar amplitudes and time constants (chloroplasts, 49 μs (61%); D-144 fragments, 90 μs (67%)) were obtained for the fast component, while the slower component differed considerably in time (chloroplasts, 2.9 ms; D-144 fragments, 170 ms). It is known that Fe-S Cluster A is photoreduced in less than 1 ms at 25 K. Data obtained support a model for Photosystem I involving a single intermediate in the decay path between the reduced primary electron acceptor (A_1^-) and $P\text{-}700^+$ and a second intermediate in the decay path between a reduced secondary electron acceptor and $P\text{-}700^+$. Dual laser-flash experiments to determine rate constants for these processes are included.

Introduction

Physiological dark-adapted (open) PS I reaction centers in chloroplasts are characterized by the primary electron donor, P-700, being reduced and all electron acceptors oxidized. Information obtained on the open state of PS I determines how the reaction center accomplishes light-induced charge separation in vivo. However, present understanding of charge separation in PS I reaction centers is primarily based upon light-induced spectroscopic changes of reaction centers in which one or more of the electron acceptors have been prereduced chemically or otherwise rendered nonfunctional [1–11].

The rise time of P-700 photooxidation in open reaction centers in detergent-treated PS I particles has been extensively studied with fast response optical systems. The initial report of less than 20 ns [12] has been revised to shorter times, from below 60 ps [9] and under 30 ps [13,14] to less than 10 ps [15]. Photoreduction of the primary electron acceptor, A_1, occurs simultaneously with P-700 photooxidation. Reduced A_1 (A_1^-) displays ab-

Abbreviations: PS, photosystem; D-144, particles, PS I particles obtained on treatment with digitonin and centrifugation at $144000 \times g$; LDAO particles, PS I particles obtained by treatment with lauryldimethylamine *N*-oxide; TSF-1, PS I particles obtained by treatment with Triton X-100; CIDEP, chemically induced dynamic electron polarization.

sorption changes which overlap with those of P-700$^+$ in the 700 nm spectral region [5]. Part of the absorption change associated with intitial charge separation decays with a time constant of 200 ps and has been interpreted to represent subsequent electron transfer from A_1^- to the secondary electron acceptor [9,13,14]. However, it has also been suggested that a reaction center triplet state, formed by recombination between A_1^- and P-700$^+$, has a similar overlapping absorption change in the 700 nm region [9]. Photoreduction of the Fe-S electron acceptor, Cluster A, has been detected optically at 430 nm, occurring in less than 100 ns [16], but the optical difference spectrum associated with the photoreduction of A_2 (Center X), the secondary electron acceptor thought to mediate electron flow from A_1 to Fe-S Cluster A, also has a band in the 430 nm region [5,17]. These overlapping optical absorption changes associated with charge separation in PS I complicate the analysis and interpretation of the spectroscopic data.

When untreated dark-adapted chloroplasts are cooled to liquid helium temperatures, PS I reaction centers remain in the open state. Low-temperature measurements of light-induced charge separation in open reaction centers are primarily limited to reversible P-700 photooxidation. In 1971, Floyd et al. [18] detected, optically at 77 K, reversible P-700 photooxidation in open reaction centers which occurred with a time constant of 30 μs. Warden et al. [19] also detected reversible photooxidation at low temperatures, however, Signal I (EPR signal of P-700$^+$) was detected to decay with a half-life of 800 ms. Recently, reversible P-700 photooxidation at low temperature was verified in open reaction centers, and was detected to occur biphasically with time constants of 122 μs and 1.7 ms at 8 K with about 80% of P-700 photooxidation being reversible [10]. In addition, photoreduction of Cluster A occurs irreversibly at temperatures less than 30 K [20]. Thus, Cluster A functions as a stable electron acceptor of PS I at these temperatures.

Of the five components presently considered to be involved in photochemical charge separation of the PS I reaction center (P-700, A_1, A_2, Center X, Cluster A and Cluster B), four have been detected in open reaction centers (P-700$^+$, A_1^-, Cluster A$^-$ and Cluster B$^-$) of spinach chloroplasts. Cluster B$^-$ is detected when chloroplasts are illuminated at higher temperatures and then lowered to 25 K for observation [21]. At 25 K, Cluster B$^-$ is detected only when Cluster A has been prereduced by illumination during freezing or by adding a chemical reductant to spinach chloroplasts before freezing. Center X (A_2) has an additional constraint: Both Cluster A and Cluster B must be prereduced by adding a strong reductant or furnishing intense illumination during freezing, or both, before Center X$^-$ is detectable in higher plants. Therefore, it remains unclear how or whether Cluster B and Center X function as obligatory electron acceptors in open PS I reaction centers at 25 K.

Measurements on primary photochemical reactions of PS I open reaction centers have been dominated by optical techniques. Conventional methods of microsecond EPR have the disadvantage of rapid-passage effects [22,23] when magnetic-field modulation methods are used. Direct detection (no modulation of the magnetic field) methods require extensive signal/averaging to achieve adequate signal-to-noise ratios. In addition, partial irreversibility of PS I at low temperature makes signal-averaged measurements difficult to accomplish. These methods of detecting kinetics are susceptible to interference from other EPR signals. In chloroplasts, a time-dependent signal of P-680$^+$ influences the kinetic traces in the g 2.0 region where Signal I (EPR signal due to P-700$^+$) occurs [24]. In addition, Singal I has been reported to show anomalous effects due to exchange interactions between P-700$^+$ and reduced electron acceptors of PS I [5,25–27]. This phenomenon, CIDEP, makes the direct analysis of Signal I on a microsecond time scale complicated and difficult to interpret.

In this study we have used EPR spectroscopy in conjuction with two lasers providing intense light flashes with microsecond time resolution, a method which is not susceptible to the problems mentioned above. This dual-laser technique has been used to determine the decay of P-700$^+$ after a 350 ns laser flash in open reaction centers at 25 K in both D-144 particles and whole chloroplasts. In addition, the rise time of Cluster A photoreduction at low temperature has been detected to be less than 1 ms. We have formulated a dynamic model

for PS I charge separation at low temperature in open reaction centers based upon kinetic data determined in this study which are consistent with optical data on open reaction centers.

Materials and Methods

Whole chloroplasts were prepared from store-bought spinach as follows [28]: Spinach leaves were disrupted for 10–20 s at 4°C in a Waring blender using the following blending solution: 0.3 M sucrose, 50 mM Tris (pH 7.8), 10 mM NaCl, and 1 mM EDTA. The mixture was filtered through four layers of filtering silk and the filtrate centrifuged at $5000 \times g$ for 2–3 min. The pellet, which contains whole chloroplasts, was resuspended in the blending solution.

To obtain D-144 particles, chloroplasts were suspended in 60 ml of 50 mM potassium phosphate, pH 7.2, and 20 mM NaCl. 20 ml of 2% digitonin (Sigma Chemical Co., No. D-5628) solution were added to the chloroplast solution and stirred slowly for 30 min at 4°C. This solution was then centrifuged at $50\,000 \times g$ for 30 min; the pellet was discarded. The supernatant was then recentrifuged for 1 h (4°C, $144\,000 \times g$). The pellet of D-144 particles was resuspended in buffer solution: 300 mM sucrose, 50 mM Tris (pH 7.8), 10 mM NaCl, 10 mM sodium ascorbate, 1 mM NaEDTA (pH 7.8) and 2 mg/ml of bovine serum albumin (Sigma Chemical Co., No A-4378).

For the poly(vinyl alcohol) preparation: 2 g of poly(vinyl alcohol) (Polysciences Inc., No. 4398) was mixed with 4 ml of 500 mM ethylene glycol. The mixture was constantly stirred while heating. The mixture is cooled and 4–6 ml of photosynthetic sample (D-144 particles or chloroplasts) added. The mixture is stirred slowly until homogeneity is obtained. The sample is then centrifuged at 12000 rpm for 1–2 min to separate unmixed poly(vinyl alcohol) and bubbles from the mixture. The poly(vinyl alcohol) sample is poured upon a smooth drying surface and placed in a desiccator with Drierite and then stored in the dark at 4°C until the poly(vinyl alcohol) film has dried to a uniform thickness of 1 mm or less, a process which takes 24–48 h. When dried, the poly(vinyl alcohol) films are cut into strips ($2–3 \times 40$ mm) to fit an EPR tube. For low-temperature EPR measurements, the EPR tubes are flushed with helium gas to provide good thermal conductivity.

Poly(vinyl alcohol) samples offer a distinct advantage for low-temperature illumination studies, since they freeze as a clear glass at temperatures down to 10 K. In addition, the EPR tube could be loaded directly in the EPR cavity without prefreezing, a process which avoids frost interference with illumination. Poly(vinyl alcohol) films are more resistant to freeze-thaw damage than chloroplasts suspended in solutions. Under repeated freeze-thaw cycles (30–40 times), freezing in liquid nitrogen and thawing in ice-cold water, the chloroplasts in solution showed diminishing light-induced EPR signal amplitudes (Signal I), while the poly(vinyl alcohol) film signals were essentially unaffected (less than 10%).

X-band EPR spectra were obtained using a homodyne EPR spectrometer operating at a frequency of 9.20 GHz. Samples were loaded into a cylindrical-mode (TE_{011}) EPR cavity (JEOL UCX-2), with a loaded quality factor (Q_L) of approx. 5000. First-derivative EPR spectra were obtained using 100 kHz magnetic field modulation, and modulation amplitudes for Signal I were set at $3.2 \cdot 10^{-4}$ T. Microwave power levels in the range of microwatts were precisely set by the use of a power meter (HP, model 432A) and an absorptive PIN diode (General Microwave Corp., model No. D-1958). Spectra were signal averaged by using a digital computer (PDP-8/L). For signal to noise improvement, the previously used klystron microwave source and Schottky-barrier detector diode were replaced by a Gunn effect oscillator (Varian, model No. VSX-9001 TZ) and a double-balanced mixer (RHG Electronics Laboratories Inc., DM8-12B) was used as a homodyne detector. Tuning of the EPR spectrometer was accomplished by critically coupling the loaded cavity with the microwave source by minimizing the monitored reflection power from the cavity.

Low-intensity (10^9 photons/cm^2 per s) illumination was obtained with a 300 W quartz-iodine lamp (General Electric Co.); fiber optics were used to carry light to the EPR cavity. High-intensity light was obtained from two coaxial flashlamp-pumped dye lasers (Phase-R Co., models DL-1100 and DL-1000). These lasers give single laser light pulses of 350 ns (full-width at half-max-

imum). For all experiments the following laser dye solution was used: 50 μM oxazine 170 perchlorate (Eastman laser grade, No. 14375), 100 μM rhodamine 6G (Eastman laser grade, No. 10724), 0.01% Triton X-100 and reagent-grade methanol as solvent. The bandwith of the laser pulse (measured with a 1-m Czerny-Turner scanning spectrograph, Jarrell-Ash Co., model 78–460) was 10 nm, centered at 690 nm. To reduce beam divergence, the flat 99% reflectance mirror was replaced by a 1 m radius concave reflector. The output of a single laser-pulse, at the end of the fiber optics, was measured by an energy meter (Hadron Inc., 102C and Gen Tec Inc., ED-200) to be approx. 20–30 mJ. For quantitative control of light intensities, solutions of $CuSO_4$ were used as optical filters at the output of the laser. The concentration of $CuSO_4$ was adjusted to obtain the desired absorbance over the bandwidth of the laser output. Fiber optics were used to transport the laser light to the microwave cavity and to the detector photodiode (SGD 100) used to detect the time delay between laser-flashes. The photodiode signal output was stored on a storage oscilloscope (Hewlett Packard, No. 1741A). A dual pulser varied the time between pulses from 1 μs to hundreds of milliseconds, and externally triggered the lasers.

Total chlorophyll concentration of photosynthetic samples was determined by the method of Arnon [29].

The ratio of Signal I spins to chlorophyll concentration was determined by comparison of Signal I intensity to an EPR standard of known spin concentration under nonsaturating EPR conditions. The following solution was used as the EPR standard [30]: 0.1 mM $CuSO_4 \cdot 5H_2O$, 2 M $NaClO_4$ and 0.01 M HCl. The relative number of spins was determined by performing a double integration of the first-derivative EPR spectrum by computer (PDP-8/L).

The microwave magnetic field intensity (H_1) in the EPR cavity decreases away from the center of the cavity. The relative sensitivity of the cavity as a function of sample depth was determined with a ruby standard. Quantitation experiments were performed with appropriate amounts of sample (approx. 1 cm height in EPR tube), such that the samples were located in the most sensitive section of the cavity. The copper standard was checked for Curie Law behavior down to 10 K, and the microwave power saturation characteristics of both Signal I and the copper standards were obtained. A low and nonsaturating microwave power, 10 μW, was used for EPR quantitation.

Optical quantitation of photo-induced P-700$^+$ was determined with an optical spectrometer (Aminco, DW-2) operating in the dual-beam model. A D-144 sample incubated with 10 mM sodium ascorbate was diluted to approx 10 μg/ml and placed in the cuvette, in the dark at room temperature. A broad-band filter (650–730 nm) was used to filter the actinic beam. In front of the photomultiplier, a broad band-pass filter (400–500 nm) was used. ΔA (435–444 nm) was used to monitor optical changes of the sample when the actinic light was turned on. Using the extinction coefficient determined by Hiyama and Ke [31] of 40 $mM^{-1} \cdot cm^{-1}$ (at 435 nm) for P-700, in D-144 particles, the ratio of P-700$^+$ to chlorophyll was determined.

The procedure for the dual laser-flash experiment was as follows: a dark-adapted sample was loaded in the EPR cavity at 25 K, and the dark EPR spectrum (see Fig. 1a) was recorded. The sample was then exposed to two high-intensity laser flashes (approx. 10^{17} photons/cm^2 per pulse, incident), with a specific time delay between the flashes. The EPR cavity was checked to make sure it was still critically coupled; if not, it was retuned. Then, the dual laser-induced EPR spectrum was recorded. The time delay between laser flashes being retained by the storage oscilloscope. This spectrum represents irreversible Signal I plus the dark spectrum (see Fig. 1b). Next, a low-intensity light source was turned on, and the EPR spectrum was recorded after maximum signal intensity was obtained (once maximal intensity was obtained turning the lamp off had no effect on signal intensity). The sample was removed from the cavity, but not from the collar assembly which holds the EPR tube, and placed in an ice-cooled beaker of water in the dark and allowed to dark adapt for 10–15 min. The EPR tube was then dried and placed back in the cavity. The orientation of the EPR tube was kept constant, such that the poly(vinyl alcohol) film was always perpendicular to the incident light beams. In this way, the sample was at the same position in the cavity for each set

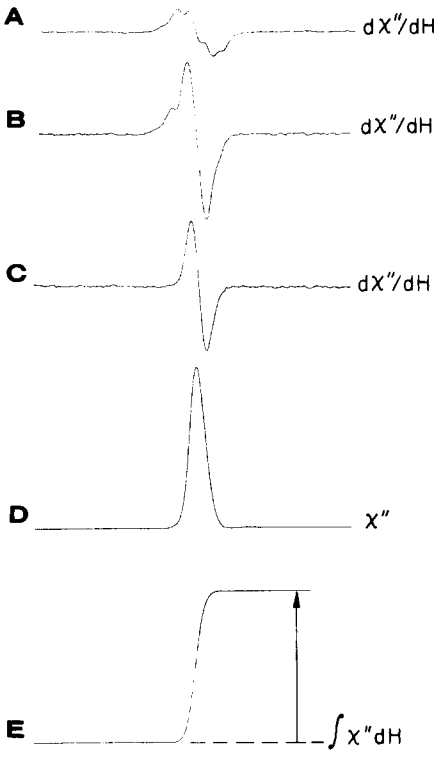

Fig. 1. EPR spectra of spinach chloroplasts. (A) First-derivative EPR signal of dark-adapted chloroplasts showing Signal II. (B) Light-induced spectrum consisting of Signal I and Signal II. (C) First-derivative light-minus-dark difference spectra, obtained by subtracting the dark spectrum from light-induced spectra, representing light-induced Signal I. (D) First integral of first-derivative signals shown in C. Represents the absorption spectrum of Signal I. (E) Second integral of C, the height of the vertical arrow represents the relative number of Signal I spins (number of P-700$^+$). EPR conditions: microwave power, 10 μW; microwave frequency, 9.20 GHz; modulation amplitude, $3.2 \cdot 10^{-4}$ T; magnetic field span, 0.3275 ± 0.01 T; temperature, 25 K.

of spectra minimizing retuning of the spectrometer after loading the sample. The dark spectrum was recorded as before. This spectrum was checked with the previous dark signals to assure that the sample had completely dark adapted. If not, the sample was removed from the cavity and again dark adapted. The above procedure was then repeated with different time delays between the laser flashes.

Curve fitting was accomplished by applying a computer program using a least-square algorithm to find the unconstrained minimum of a function whole first and second derivatives are known [32].

Results

Single laser-flash responses

Signal I. The kinetics of Signal I, in D-144 fragments at 25 K, induced by a high-intensity (approx 20 mJ) laser pulse (350 ns) was monitored by EPR. For this measurement, the EPR spectrometer was operating with 100 kHz modulation and a time response of 1 ms. The positive peak of the first-derivative signal of Signal I was monitored during laser excitation. Fig. 2 shows the results of these experiments.

The initial rise of the g 2.0 signal does not reach its maximum intensity, determined by continuous illumination, but does show a prominent decay with $t = 260$ ms. Signal I decays to an irreversible level which is approx. 40% of the maximum signal intensity obtained with continuous illumination. A second laser flash produces an irreversible Signal I intensity level which is approx 65% of the maximum signal intensity. The irreversible g 2.0 signal, induced by both continuous illumination and a single laser flash, has a linewidth of $7.5 \cdot 10^{-4}$ T which is characteristic of Signal I. Similar results were obtianed with highly enriched PS I particles (LDAO particles). However, when intact or broken chloroplasts were examined on this time scale, no Signal I kinetics were detected, but Signal I intensity was found to be 40% of the maximum after the laser flash. Presumably, the decay of Signal I is much faster in chloroplasts than in PS I particles and decays to 40% in less than 1 ms.

A maximum of 40% of the reaction (P-700, Cluster A : P-700$^+$, Cluster A$^-$) occurs irreversibly at 25 K, independent of laser-flash intensity. If the concentration of chlorophyll of the sample was lowered and the intensity of light increased, still a maximum 40% irreversible P-700$^+$ was light induced. However, if the chlorophyll concentration of the sample was increased, the maximum percentage of P-700 molecules irreversibly photooxidized, at 25 K, by a single laser flash, and independent of light intensity, was always less than 40%. This is attributed to absorbance effects; i.e., at higher chlorophyll concentrations, the laser flash is only exciting a proportion of the total reaction centers. Since all flash-induced responses are normalized to continuous illumination-induced Signal I intensity, the percentage of Signal I

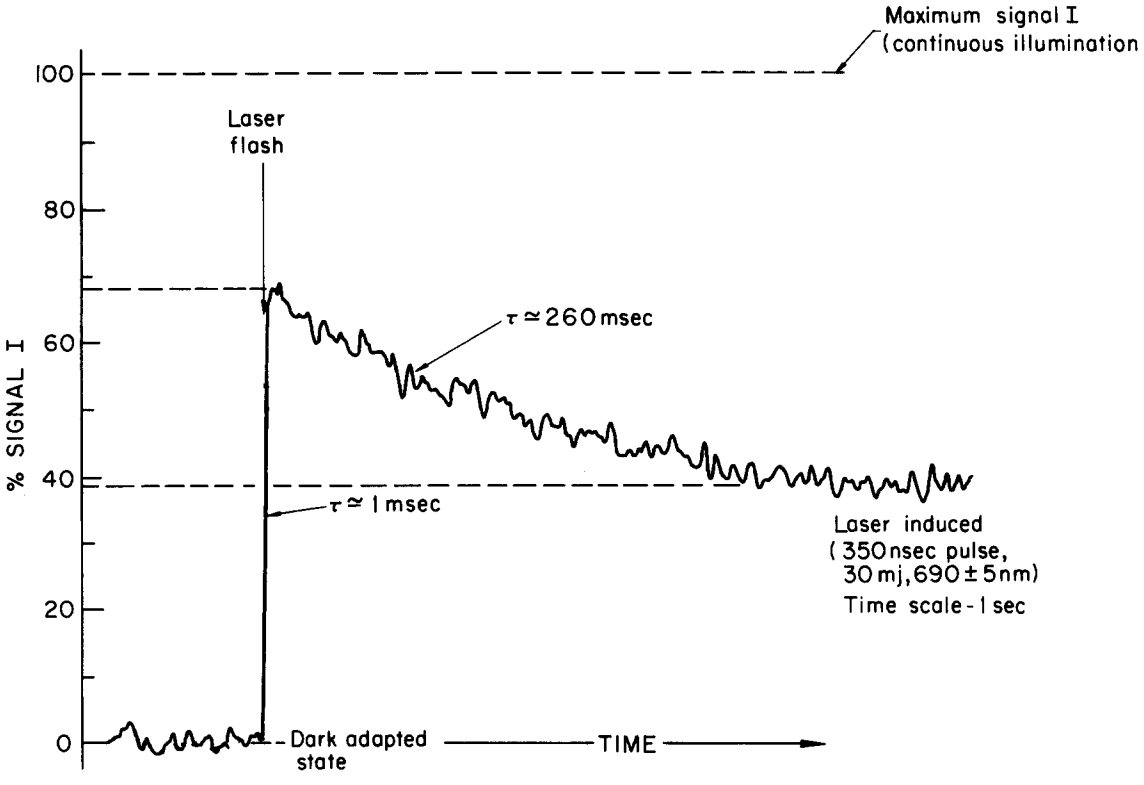

Fig. 2. Kinetic trace of the response of the positive peak of the first-derivative EPR signal of Signal I (D-144 particles) to a laser light pulse at 25 K. The horizontal line positioned at 100% represents the amplitude of the positive peak of Signal I under continuous illumination (when light is turned off, no decay is observed at 25 K). After the laser flash, Signal I decays exponentially (τ = 260 ms). Signal I decays to a signal intensity of approx. 40% of maximum, and is irreversible at this temperature. Kinetic trace represents an average of 15 experiments.

determined for a single flash will be lower because the continuous illumination represents a larger population than that initially photooxidized by a single laser flash. To ensure that the percentages presented for Signal I correspond to P-700$^+$, Signal I and P-700$^+$ induced by continuous illumination were determined relative to the total chlorophyll concentration. The ratio between Signal I at 25 K and P-700$^+$ at room temperature was determined to be $1:1 \pm 0.2$. This result is in agreement with previous quantitations comparing these signals at room temperature [33–35].

High-intensity vs. low-intensity light. The yield of irreversible P-700$^+$ photoinduced by a low-intensity light flash (approx. 15 s) was compared to that produced by a high-intensity laser-flash (350 ns) of equal energy. The results are shown in Fig. 3 where the %P-700$^+$ irreversibly photooxidized is plotted as a function of the incident illumination energy for both intensity sources. Except for very low energies, low-intensity light is much more efficient in irreversibly oxidizing P-700 than high-intensity light at 25 K [36].

Cluster A. The laser-flash-induced rise time of the *g* 1.94 EPR signal, attributed to iron-sulfur Cluster A, was monitored in dark-adapted D-144 particles at 15 K. The response time of the spectrometer was the same as that used to detect the decay of Signal I, 1 ms. The first-derivative peak of the *g* 1.94 signal was monitored when the sample was excited by a laser flash. This signal was found to rise in an irreversible manner within the time response of the spectrometer (see Fig. 4). Thus, the photoreduction of Cluster A in D-144 fragments at 15 K occurs in less than 1 ms (the same result was obtained with LDAO particles).

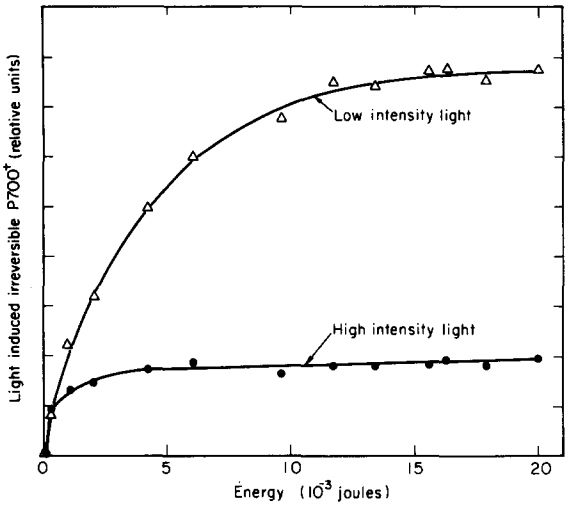

Fig. 3. The production of irreversible Signal I induced by both a high-intensity and low-intensity light source is plotted as a function of the light pulse energy (incident). The low-intensity light source was on for 15 s to obtain an energy output equal to that of a high-intensity laser pulse (350 ns).

The percentage of irreversibly photoreduced Cluster A was equal to the percentage of irreversibly photooxidized P-700$^+$. The percentage of iron-sulfur Cluster A photoreduced by a single laser flash was determined by comparing the signal intensity at g 1.94 with the maximum intensity induced by continuous or long illumination. No attempt was made to integrate the iron-sulfur cluster spectrum.

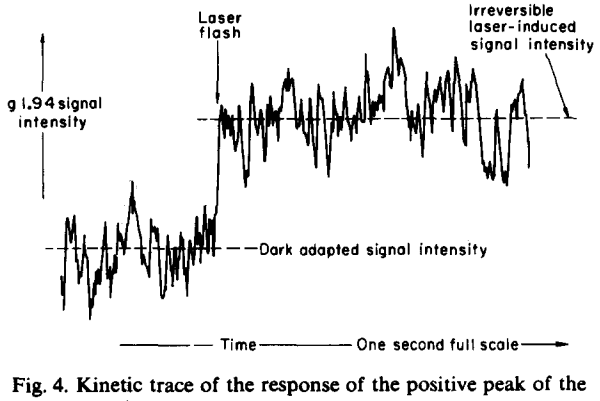

Fig. 4. Kinetic trace of the response of the positive peak of the first-derivative EPR signal of iron-sulfur Cluster A at g 1.94. When exposed to a laser flash the signal intensity of g 1.94 increases irreversibly. The rise time of this signal is within the time response of the spectrometer, less than 1 ms. This trace represents the response to a single laser flash at 15 K.

Dual laser-flash response

Dual laser-flash experiments were performed, in which the signal intensity of irreversible Signal I produced by two laser flashes was determined as a function of the delay time between flashes, at 25 K. These experiments were performed on D-144 fragments and chloroplasts. The results are plotted on the graph shown as Fig. 5.

The ordinate of Fig. 5 represents the percentage of Signal I irreversibly photooxidized by two laser flashes. The log of the delay time between these laser flashes is shown on the abscissa which ranges from 1 μs to 1 s. For each point on the plot, three EPR spectra were needed; dark, dual laser-flash-induced signal, and continuous low-intensity light-induced signal. The percentage of Signal I induced by dual laser flashes was determined by double integration of light-dark spectra obtained by subtraction of the dark spectra from the dual laser-flash spectra, and then dividing it by the value obtained by double integration of the continuous light-minus-dark spectra (see Fig. 1).

The results of dual laser-flash experiments show that the effectiveness of two laser flashes, at 25 K, in photoinducing irreversible P-700$^+$ in chloroplasts and D-144 particles, is a sensitive function of the delay between the laser flashes. When the laser flashes are administered simultaneously, the production of irreversible P-700$^+$ is equivalent to that produced by a single laser flash. This ensures that a single laser light pulse is saturating the reaction centers. Maximum yield of irreversible P-700$^+$ is achieved when the laser pulses are far apart. The exact time range depends upon the preparation. For D-144 fragments, the time between flashes (greater than 170 ms) had to be about 100-times longer than for chloroplasts (greater than 2.9 ms) for maximum irreversible P-700$^+$ yield!

The time dependence for the production of irreversible P-700$^+$ can be fit by a function containing two exponentials:

$$\text{P-700}^+(t)_{\text{irrev.}} = \text{P-700}^+(\infty) - \left[X_1 \exp\left(-\frac{t}{\tau_1}\right) + X_2 \exp\left(-\frac{t}{\tau_2}\right)\right] \times [\text{P-700}^+(\infty) - \text{P-700}^+(0)] \quad (1)$$

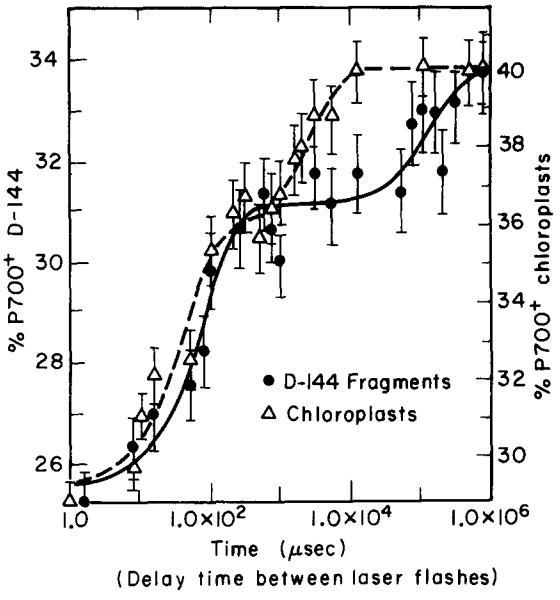

Fig. 5. Results of the dual laser-flash experiment. Each point represents the percentage of Signal I which is photoinduced by two laser pulses with the delay time between the pulses presented on the abscissa. The vertical bars represent an error of ±3% in determining the intensity of Signal I. The solid and dotted lines represent a least-squares computer fit of the data. (See Table I, for best-fit parameters.) The actual values measured are shown to the left and right of the plot for D-144 particles and chloroplasts, respectively. The abscissa represents time on a log scale, spanning over six orders of magnitude from 1 μs to 1 s.

Where P-700$^+$ (∞) represents the maximum yield of irreversible P-700$^+$ obtained by two laser flashes (delay time, $t = \infty$). When two flashes are simultaneously given ($t = 0$) the minimum yield is obtained and is equal to that produced by a single laser flash. Fig. 5 shows the results of the dual laser-flash experiments and the fit of Eqn. 1 (dotted and solid lines). The parameters X and τ of Eqn. 1 are shown in Table I for the respective samples.

TABLE I

VALUES OBTAINED BY BEST-FIT COMPUTER ANALYSIS OF THE DUAL LASER-FLASH EXPERIMENT

Sample	τ_1 (ms)	X_1	τ_2 (μs)	X_2
D-144 particles	170	0.33±0.1	91	0.67±0.1
Chloroplasts	2.9	0.39±0.1	49.3	0.61±0.1

Discussion

The result of the dual-flash experiments is that the yield of stable charge separation (P-700, Cluster A: P-700$^+$, Cluster A$^-$) at 25 K is dependent upon the delay between two laser flashes. There are three possible origins for the delay time dependence; high-intensity light-induced effects in the chlorophyll antenna complexes, electron reduction of P-700$^+$ associated with the electron-transport system mediated by plastocyanin, and elctron reduction of P-700$^+$ due to charge recombination in the PS I reaction center. It will be shown that charge recombination is exclusively responsible for the time constants detected in the dual-laser experiments. These time constants will be used to develop a model for reversible charge separation in PS I at 25 K.

The incident laser light intensities (10^{17} photons/cm^2 per flash) used in the dual-laser experiments exceed the threshold (10^{13} photons/cm^2 per flash absorbed) for high-intensity light-induced effects in antenna systems of chloroplasts [37,38]. Therefore, high-intensity light-induced processes are most probably occuring in chlorophyll antenna systems. As Fig. 3 shows, high-intensity light is not as effective as low-intensity in producing stable charge separation and this effect is partially due to high-intensity light-induced antenna phenomena. The mechanisms involved in the antenna are dependent upon the length of the high-intensity light pulse. For microsecond laser pulses (350 ns laser pulses were used for the dual-laser experiments) the predominant mechanism involves relatively long-lived (5 μs) exciton quenching species [39]. The involvement of long-lived quenchers may influence the time dependence detected in the dual laser-flash experiment. However, time constants detected in these experiments were an order of magnitude longer than the lifetime of the quenching species (shortest time constant detected was 49 μs, See Table I). In addition, the long-lived quenchers would have to quench excitation before it reaches P-700 with an extremely high efficiency. Therefore, we conclude that high-intensity light-induced effects in the antenna complexes do not influence the results of the dual laser-flash experiments.

At room temperature plastocyanin is known to

function as an electron donor to P-700$^+$ [40,41]. However, plastocyanin displayed no photoinduced activity at low temperature when measured on a millisecond time scale. This was determined by monitoring the g 2.05 signal of plastocyanin during flash excitation at 25 K. In addition, there is no evidence of any other secondary donor to P-700$^+$ functioning at low temperature. In any case, the percentage of Fe-S Cluster A irreversibly photoreduced at 25 K was equal to the percentage of Signal I irreversibly photooxidized. Thus, it is clear that stable charge separation is obtained by the irreversible nature of reduced Cluster A at low temperature.

The time constants detected in the dual laser-flash experiments represent charge recombination between P-700$^+$ and reduced electron acceptors. When the laser pulses are delayed far apart in time, excitation due to the first laser pulse produced charge separation with 40% of the reaction centers forming an irreversible charge separation state while the remaining 60% undergo recombination with P-700$^+$. Excitation from the second laser pulse reexcites the 60% which have undergone reversible charge separation and 40% of these reaction centers (24%) form a stable charge-separation state netting a total of 64% of the reaction centers with irreversibly oxidized P-700$^+$. When the delay time between the two laser flashes is decreased some of the reaction centers will not complete recombination processes between the laser flashes and will not be involved with further charge separation induced by the second laser. Thus, the number of reaction centers forming stable charge-separation will decrease. By carefully examining the delay time dependence with respect to production of stable charge separation the dynamics of the charge-recombination process is elucidated.

The time dependence for charge recombination in chloroplasts and D-144 particles is shown in Fig. 5. In the case of D-144 particles the time dependence is best modeled by two exponentail components. The time constants are sufficiently separated such that a substantial plateau is evident (see solid line, Fig. 5). In support of this interpretation is the stoichiometric agreement between continuous illumination, single laser-flahs and dual laser-flash-induced P-700$^+$. Quantitation of Signal I with P-700$^+$ has shown that Signal I induced by continuous illumination represents the total P-700 population. 40% of the total P-700 is irreversibly photooxidized by a single laser flash and a slow component is responsible for 40% ($\{65 - 40\}/\{100 - 40\}$) of the P-700$^+$ recombination processes in D-144 particles (see fig. 2). Assuming biphasic decay, the other component in P-700$^+$ decay (charge recomibination) must be faster and represent 60% of recombination. Table I shows the dual laser-flash data and predicts that only two significant kinetic components are involved with recombination and the slower component reflects 33% while the faster reflects 67% of charge recombination in D-144 particles. The agreement between these values determined from single- and dual-laser excitation strongly supports our explanation for the data and in addition eliminates the possibility of a significant faster component involved with P-700$^+$ charge recombination.

In the case of chloroplasts the data of Fig. 5 are not adequate to choose a priori between monophasic or biphasic time dependence. However, the data of Fig. 5 do suggest biphasic behavior. Like the D-144 particles, when chloroplasts are exposed to a single laser flash, 40% of the P-700 population is irreversibly photooxidized. Thus, the forward charge-separation yield is not altered when D-144 particles are isolated from chloroplasts. The decay of P-700$^+$ after a laster flash is too fast to be monitored by millisecond EPR, but the extent of irreversible charge separation is the same as for D-144 particles, 40%. The results of the dual laser-flash experiments predict such a behavior (see Fig. 5). We favor biphasic charge recombination in chloroplasts (dotted line, Fig. 5). This is based upon the biphasic behavior of D-144 recombination. It is possible that treating the chloroplasts with digitonin could alter charge-recombination pathways, but this seems unlikely since the forward yield is unaltered. Examination of Table I shows that the amplitude factors for the exponentials are approximately the same for chloroplasts and D-144 particles. Thus, if our conclusions are correct, the dominant decay route (faster component) is the same for chloroplasts and D-144 particles as the precision for τ values is, such that they could be equal. As for the slower components, the magnitude of the effect is unaltered but in D-144 particles this component is much slower. Assum-

ing the forward rates are unaltered, a model for PS I must be able to account for equal forward yields and a difference in recombination rates. Finally, in support of our interpretations are the results of Mathis and Conjeaud [10] who detected optically, at 820 and 703 nm, biphasic decay of P-700$^+$ (τ of 122 μs and 1.7 ms), after a laser flash in chloroplasts at 8 K. Table I shows our results determined by fitting Eqn. 1 to the dual-laser data, and reveals time constants (49 μs and 2.9 ms) for chloroplasts which are similar to the results of Mathis and Conjeaud. However, the amplitudes (X_1 and X_2) of these components differ considerably. They found that the fast component dominated the decay at 8 K while we find that both components are significant in the decay at 25 K. We also find similar amplitude factors for P-700$^+$ decay in D-144 fragments (see Table I). They have also reported that P-700$^+$ decays by 80%, while we have clearly shown that P-700$^+$ decays maximally by 60%.

Model for PS I charge recombination

Three models for PS I charge separation will be presented which are consistent with the kinetic measurements made in this study [42]. Only components detected in open reaction centers will be used explicitly in these models: P-700, A_1 and Cluster A. The starting state for kinetic analysis is the state; P-700$^+$, A_1^- and any other electron acceptors oxidized. At time zero, the electrons proceed from A_1^- depending upon the relative values of the rate constants for the reaction pathways shown in the models.

$P(1)^R$ of model I (see Fig. 6) represents a recombination product between the reduced primary electron acceptor A_1^- and the oxidized primary electron donor P-700$^+$, and is shown as an intermediate in the decay path between A_1^- and P-700$^+$. Model I predicts biphasic recombination with P-700$^+$. In consideration of the time for photoreduction of Cluster A (less than 1 ms) and the values of the two time constants detected for P-700$^+$ recombination (91 μs and 170 ms) in D-144 particles, the 170 ms time constant must represent the lifetime of the recombination product, $P(1)^{R-}$.

Model II (see Fig. 6) differs from model I in that a secondary electron acceptor (Z) functions to mediate forward charge separation between A_1 and Cluster A. Model II predicts triphasic decay of P-700$^+$ [42]. However, if the decay of A_1^- is much faster then the decay of the reduced secondary acceptor, Z^-, and the lifetime of the recombination product $P(1)^{R-}$, the reduction of P-700$^+$ will be biphasic. Similar to model I, the 170

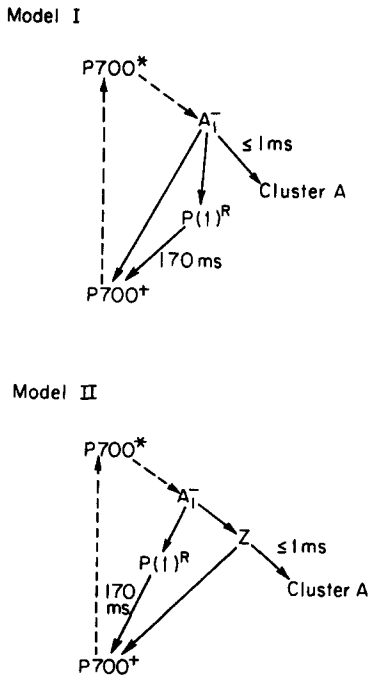

Fig. 6. Kinetic models for PS I charge separation. $P(1)^R$ represents a recombination product (see text).

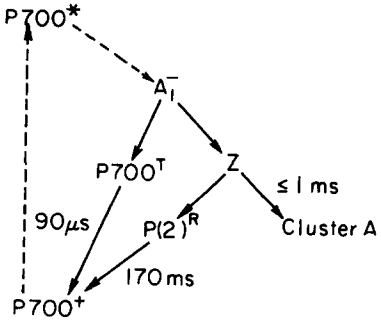

Fig. 7. Proposed kinetic model for PS I charge separation and recombination. Kinetic parameters measured in this study are assigned as shown. P-700^T represents a triplet state and $P(2)^R$ a recombination product (see text). The time constants are those determined in this study.

ms time constants must represent the lifetime of the recombination product, $P(1)^{R-}$.

Both models I and II are consistent with the kinetic data determined in this study and cannot be ruled out as valid models for PS I charge separation solely on the basis of these measurements. However, in consideration of information obtained about $P(1)^R$ from partly closed reaction centers these models do not seem appropriate. Shuvalov et al. [9] who monitored, optically, reversible charge separation in TSF-1 particles in which the only functional electron acceptor is A_1, observed two kinetic components in the 700 nm spectral region which were interpreted to represent the rise and decay of a recombination product between A_1^- and P-700$^+$. At room temperature the two time constants were 10 ns and 3 μs. When the temperature was lowered to 5 K the 3 μs time constant increased to 1 ms. In addition, when the reducing conditions were adjusted such that only Clusters A and B were prereduced the time constants did not change. Another report of a recombination product existing between A_1 and P-700 is in the work of Frank et al. [2] who detected a photoinduced triplet state of P-700 which was thought to be formed by recombination when Center X was prereduced. This has recently been supported by McLean and Sauer [8]. In addition, Setif et al. [11] also concluded that the recombination product between A_1^- and P-700$^+$ is a triplet state of P-700. Therefore, it seems that $P(1)^{R-}$ is a triplet state formed by recombination between A_1^- and P-700$^+$. Both models I and II predict that the lifetime of this triplet state is 170 ms which is relatively long for a chlorophyl triplet state and much longer than the lifetime of this state reported by both Shuvalov et al. [9] (1 ms) and Setif et al. [11] (800 μs at 10 K). Therefore, the most appropriate model for PS I charge separation is shown here as model III (see Fig. 7).

Model III differs from previous models in that two distinct recombination products are formed between P-700$^+$ and two reduced acceptors. $P(2)^R$ is an intermediate in the recombination path between the secondary electron acceptor (Z) and P-700$^+$. This model predicts that the time dependence of P-700$^+$ decay will involve four exponentials [42]. However, if the decay of A_1^- is much faster than the decay of $P(1)^{R-}$ (triplet state of P-700, P-700^1) and the decay of Z^- much faster than the lifetime of $P(2)^{R-}$, then recombination with P-700$^+$ will be biphasic. If model III is appropriate and the above assumptions valid then the lifetime of P-700^T is 50–90 μs in both D-144 particles and chloroplasts and the lifetime of $P(2)^{R-}$ is 170 ms in D-144 particles and 2.9 ms in chloroplasts. In addition, the branching ratio in D-144 particles for reverse electron flow back to P-700$^+$ from A_1^- is 0.40 (chloroplasts, 0.37) and from the secondary electron acceptor Z^- 0.33 (chloroplasts, 0.37). Notice that the branching ratios for chloroplasts and D-144 particles are approximately the same. The difference in half-life of the slower decay component between chloroplasts and D-144 particles can be explained by considering only the lifetime of $P(2)^{R-}$ as the forward charge-separation process is equivalent in both preparations.

This is the first report in which an intermediate state, $P(2)^R$, is found to function in the decay path from a secondary electron acceptor. Center X (A_2) is only observed when Cluster A and B are prereduced. The kinetics of Center X^- have been detected at low temperature and in TSF-1 particles. Shuvalov et al. [5] reported that the rise time for the photoreduction of Center X^- is less than 200 μs, and that it decays in 130 ms. In addition, one of the exponential decay components of P-700$^+$ was detected with the same time constant as Center X^- decay. Thus, it appears that Center X^- is directly back-reacting with P-700$^+$. A direct correlation between Center X^- and P-700$^+$ decay was also observed by McIntosh et al. [1] with $\tau = 800$ ms. In terms of model III, this would be a characteristic of $P(2)^R$. Because the time constant for the photoreduction of Cluster A is less than 1 ms, it is clear that Center X^- decays too slowly to be involved in forward photochemistry of PS I, if the values, reported for Center X^- decay when Cluster A and B are reduced, reflect the decay of Center X^- when A and B are available for electron transfer! There is a striking similarity in the decay time detected in this work (170 ms) and that reported for Center X^- decay (130 ms [5] and 800 ms [1]). If the decay of Center X^- does not change significantly when Clusters A and B are not prereduced then $P(2)^{R-}$ can be assigned to this center. If this is the case then Cluster B or a previously

undetected component is the secondary electron acceptor, Z. In light of the recent work of Chamorovsky and Cammack [21], Cluster B functions as a stable electron acceptor similar to Cluster A and does not seem to be a good candidate for the secondary electron acceptor. Alternatively, if the decay of A_2 (Center X) is significantly accelerated by opening the reaction center then it can be assigned as the secondary electron acceptor and the recombination product, $P(2)^R$, represents a new recombination intermediate.

Conclusion

This work questions the validity of the assignment of Center X (A_2) as the secondary electron acceptor of PS I, based solely upon information obtained from partly closed reaction centers. Until the rise and decay kinetics of Center X (A_2) are measured when Clusters A and B are available for electron transfer, the function of Center X in charge separation of PS I remains unclear.

It has been suggested that chloroplasts contain kinetically different PS I reaction centers [43]. If this was the reason for the differences between D-144 particles and chloroplasts recombination kinetics, we would expect the chloroplasts to exhibit the slower kinetics, since D-144 particles are thought to be derived from the stroma lamallae of chloroplasts. Thus, the slower recombination kinetics of D-144 particles may be due to a detergent-induced effect.

The phenomenon of low-intensity light being more effective than high-intensity light in photoproducing stable charge separation in PS I at 25 K can be explained by considering both high-intensity antenna effects and reversible charge separation. A saturating high-intensity laser flash produces a single-turnover event with respect to charge separation (rate of recombination is much slower than the 350 ns laser flash, see Table I) producing a maximum of 40% stable charge separation. A low-intensity flash of equal energy will turn over PS I many times increasing the proportion of reaction centers which attain stable charge separation. In addition, a saturating low-intensity excitation will not induce exciton-exciton annihilation processes in the chlorophyll antenna matrix.

Acknowledgments

We would like to thank Robert Goldstein, Kenneth Sauer, and Richard Malkin for helpful discussions. We would also like to thank Richard Malkin for the LDAO particle samples. This work is supported through research support from the National Science Foundation (Biophysics Research Program, PCM 7822245) and the Department of Energy through the Division of Biology and Medicine of the Lawerence Berkeley Laboratory. We are highly indebted to C.S. Schenck and W.W. Parson of the University of Washington for suggesting the use of poly(vinyl alcohol) films.

References

1 McIntosh, A.R., Chu, M. and Bolton, J.R. (1975) Biochim. Biophys. Acta 376, 308–314
2 Frank, H.A., McLean, M.B. and Sauer, K. (1979) Proc. Natl. Acad. Sci. U.S.A. 76, 5124–5128
3 Shuvalov, V.A. (1976) Biochim. Biophys. Acta 430, 113–121
4 Sauer, K., Mathis, P., Acker, S. and Van Best, J.A. (1978) Biochim. Biophys. Acta 503, 120–134
5 Shuvalov, V.A., Dolan, E. and Ke, B. (1979) Proc. Natl. Acad. Sci. U.S.A. 76, 770–773
6 Mathis, P., Sauer, K. and Remy, R. (1978) FEBS Lett. 88, 275–278
7 Sauer, K., Mathis, P., Acker, S. and Van Best, J.A. (1979) Biochim. Biophys. Acta 545, 466–472
8 McLean, M. and Sauer, K. (1982) Biochim. Biophys. Acta 679, 384–392
9 Shuvalov, V.A., Ke, B. and Dolan, E. (1979) FEBS Lett. 100, 5–8
10 Mathis, P. and Conjeaud, H. (1979) Photochem. Photobiol. 29, 833–837
11 Setif, P., Hervo, G. and Mathis, P. (1981) Biochim. Biophys. Acta 638, 257–267
12 Witt, K. and Wolff, C. (1970) Z. Naturforsch 25b, 387–388
13 Shuvalov, V.A., Klevanik, A.V., Sharkov, A.V. and Kryukov, P.G. (1980) Dokl. Akad. Nauk S.S.S.R. (English Translation) 248, 756–759
14 Shuvalov, V.A., Klevanik, A.V., Sharkov, A.V., Kryukov, P.G. and Ke, B. (1979) FEBS Lett. 107, 313–316
15 Fenton, J.M., Pellin, M.J., Govindjee and Kaufmann, K.J. (1979) FEBS Lett. 100, 1–4
16 Ke, B. (1972) Arch. Biochem. Biophys. 152, 70–77
17 Hiyama, T. and Fork, D.C. (1980) Arch. Biochem. Biophys. 199, 488–496
18 Floyd, R.A., Chance, B. and DeVault, D. (1971) Biochim. Biophys. Acta 226, 103–112
19 Warden, J.T., Mohanty, P. and Bolton, J.R. (1974) Biochem. Biophys. Res. Commun. 59, 872–878
20 Ke, B., Sugahara, K., Shaw, E.R., Hansen, R.E., Hamilton, W.D. and Beinert, H. (1974) Biochim. Biophys. Acta 368, 401–408

21 Chamorovsky, S.K. and Cammack, R. (1982) Biochim. Biophys. Acta 679, 146–155
22 Portis, A.M. (1955) Technical note No. 1, Sarah Mellon Scaife Radiation Laboratory, University of Pittsburgh
23 Weger, M. (1960) Bell Syst. Tech. J. 39, 1013–1112
24 Malkin, R. and Bearden, A.J. (1973) Proc. Natl. Acad. Sci. U.S.A. 70, 294–297
25 Dismukes, G.C., McGuire, A., Blankenship, R. and Sauer, K. (1978) Biophys. J. 21, 239–256
26 Friesner, R., Dismukes, G.C. and Sauer, K. (1979) Biophys. J. 25, 277–294
27 McIntosh, A.R. and Bolton, J.R. (1976) Nature 263, 443–445
28 Kalberer, P.P., Buchanan, B.B. and Arnon, D.I. (1967) Proc. Natl. Acad. Sci. U.S.A. 57, 1542–1549
29 Arnon, D.L. (1949) Plant Physiol. 24, 1–15
30 Malmström, B.G., Reinhammer, B. and Vänngård, T. (1970) Biochim. Biophys. Acta 205, 48–57
31 Hiyama, T. and Ke, B. (1972) Biochim. Biophys. Acta 267, 160–171
32 Gill, P.E., Murry, W., Picken, S.M. and Gould, N.I.M. NPL Library, Lawrence Berkeley Laboratory
33 Baker, R.A. and Weaver, E.C. (1973) Photochem. Photobiol. 18, 237–240
34 Warden, J.T. and Bolton, J.R. (1973) J. Am. Chem. Soc. 95, 6435–6436
35 Warden, J.T. and Bolton, J.R. (1972) J. Am. Chem. Soc. 94, 4352–4353
36 Bearden, A.J. and Malkin, R. (1976) Biophys. J. 16, 160a
37 Mauzerall, D. (1976) Biophys. J. 16, 87–91
38 Geacintov, N.E., Breton, J., Swenberg, C.E. and Paillotin, G. (1977) Photochem. Photobiol. 26, 629–638
39 Breton, J., Geacintov, N.E. and Swenberg, C.E. (1979) Biochim. Biophys. Acta 548, 616–635
40 Haehnel, W. (1977) Biochim. Biophys. Acta 459, 418–441
41 Bouges-Bocquet, B. (1977) Biochim. Biophys. Acta 462, 362–370
42 Crowder, M.S. (1981) Dissertation, University of California, Berkeley
43 Rurainski, H.J., Gerhardt, R. and Mader, G. (1982) Z. Naturforsch. 37c, 31–39